A Diesel-Powered Fuel Cell APU—Reliability Issues and Mitigation Approaches

Boštjan Pregelj, Andrej Debenjak, *Member, IEEE*, Gregor Dolanc, and Janko Petrovčič

***Abstract*—The paper deals with reliability issues of a diesel-powered fuel cell auxiliary power unit (APU). The unit combines an autothermal diesel reformer and a proton exchange membrane fuel cell stack. The focal point is mitigation approaches for increasing the reliability of the complete APU system. These include control strategies on the one side, and electronic hardware solutions on the other. The measures, guarantying safe, reliable, and long-life operation, were developed, implemented and experimentally validated on a 3-kW net electric power APU system targeted for truck on-board applications.**

***Index Terms*—Fault protection, fault-tolerant control design, fuel cells, fuel processing, power conversion, power generation.**

I. Introduction

THE proton exchange membrane (PEM) fuel cell technology provides high-efficiency energy conversion, with low pollutant emissions and silent operation [1], [2]. These features represent the main driving force behind fuel cell systems designed to be used as auxiliary power unit (APU) in mobile applications, such as trucks, caravans, and yachts. However, in its basic principle, PEM fuel cells operate with hydrogen rather than with ubiquitous hydrocarbon fuels.

Reforming technology has been brought in to cope with the not yet adequately formed hydrogen infrastructure [3]. Moreover, it offers a solution where no infrastructure is available, as with remote areas and special transportation and maritime applications. However, the reforming technology introduces additional complexity compared to bare hydrogen fuel cell systems [4]–[7]. The resulting systems consist of complex chemical reactors featuring a number of reactions, a high degree of interaction, substantial temperature differences, and high energy density. A comprehensive portfolio of supporting subsystems is a prerequisite for optimal exploitation of such a technology. The portfolio includes numerous balance of plant (BoP) components, a diverse list of sensors, power conditioning components, battery, and control unit. Consequently, if the increased complexity is not handled effectively, the reliability of the complete system is compromised.

A few reforming-based APU prototype systems have been developed recently [8]–[11]. These systems are targeting truck, maritime, and remote-area applications. The developed systems prove the technology works; and, its green appeal is important for further commercialization. Furthermore, by exploiting the residual heat, its potential even increases. However, these prototypes also point to several unresolved issues in design (e.g., component certification and BoP components availability) and usage (high costs, modest reliability, serviceability, and system life-time). These issues have to be resolved prior to successful commercialization and deployment of the technology.

Reliability and expected life-time of such systems can be improved by avoiding degradation phenomena and damaging events. Beside system design approaches for minimizing the risk of such events, effective operation management and control is of critical importance. The main targets of such a control system are twofold: 1) keeping the process parameters at optimum or within a predefined range under all operation modes, and 2) detecting, preventing, or mitigating the harmful events.

Designing such a control system is a challenging task due to the high complexity of the underlying reformer-fuel-cell setup and the absence of in-detail knowledge of all the phenomena that can occur inside any individual reactor. Studies managing the operation of *complete real systems* and comprising a series of reactors are limited in number [12], [13], with only a few discussing specific operation procedures such as startup [14], [15]. On the other hand, interesting simulation studies on control design can be found for methane [16], methanol [17], and diesel [18] fuel processors. Whereas, most of the studies presenting mitigation approaches treat a *single* reactor case, predominantly with model-based verification (for example [19]). Moreover, an example of small-scale catalytic partial oxidation (CPOX) fuel processor implementation is discussed in [20].

This paper discusses control strategies and electronic hardware solutions for increased reliability and prolonged life-time of an APU system comprising a diesel reformer, PEM fuel cell stack and battery. The presented solutions are based on our recent experience in hydrogen technologies [21]–[26] and were developed within the EU FP7 FCGEN Project [10], [27]–[30]. Beside the sole control tasks, several additional operation issues with degrading or fatal effect to the system have been identified and addressed. The innovative value of this paper is in the

Manuscript received September 16, 2016; revised December 12, 2016; accepted December 22, 2016. Date of publication February 24, 2017; date of current version July 10, 2017. This work was supported in part by the European Union's Seventh Framework Program (FP7/2007-2013) for the Fuel Cells and Hydrogen Joint Technology Initiative under Grant 277844 and in part by the Slovenian Research Agency through the Research Program P2-0001.

The authors are with the Department of Systems and Control, Jožef Stefan Institute, SI-1000 Ljubljana, Slovenia (e-mail: bostjan.pregelj@ijs.si; andrej.debenjak@ijs.si; gregor.dolanc@ijs.si; janko.petrovcic@ijs.si).

Color versions of one or more of the figures in this paper are available online at http://ieeexplore.ieee.org.

Digital Object Identifier 10.1109/TIE.2017.2674628

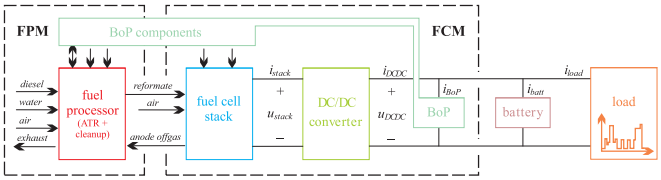

Fig. 1. Main APU's components, reactant flows, and electric connections.

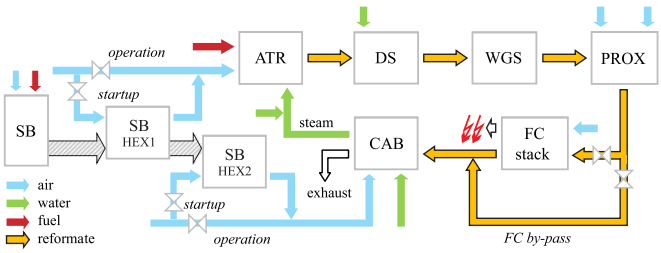

Fig. 2. Fuel-processing reactors and process flows (without cooling). SB with HEX1 and HEX2, ATR, DS, WGS, PrOx, fuel cell stack (FC), CAB.

extent of *control means that consider the overall system*. The embedded solutions take into account as much information about the system state as possible (temperatures, reactant flows, measurable disturbances, component failures, electric load, etc.) and apply appropriate coordinated action. This way, autonomous, safe, and long-term operation of the APU system is ensured.

The paper is organized as follows. In Section II, the diesel fuel cell APU system is described. The harmful phenomena and the mitigation strategies are discussed in Section III and the complementary electronic hardware solutions in Section IV. Finally, Section V gives a general conclusion on the presented solutions.

II. Diesel-Powered Fuel Cell APU

A diesel-powered fuel cell APU consists of the following two main subsystems (as shown in Fig. 1):

1) a diesel fuel processor module (FPM); and
2) a fuel cell and electric power module (FCM).

The operation of such a system is made possible by numerous BoP components, power management and conditioning subsystems, and an electronic control unit (ECU). Furthermore, a battery is an essential part of the system. It provides power for startup and shutdown procedures, and covers energy shortage or excess during sudden load transients.

A. Diesel-to-Electricity Process

The diesel-to-electricity conversion process is divided into two steps. The first one is the *chemical diesel-to-hydrogen conversion*, and the second being the *electrochemical hydrogen-to-electricity conversion*. The first takes place in the diesel fuel processor module, and the second in the fuel cell stack. The scheme of the process is presented in Fig. 2.

The basis of the diesel fuel processing technology is the reforming process. The fuel processor at hand is based on the autothermal reformer (ATR) [31]. Compared to other technologies such as CPOX [20] and steam-reforming [3], [5], the ATR is a combination of both. The energy required for the endothermic reforming process is released by the exothermic partial oxidation of diesel molecules in the very same reactor. This way the heat transfer is maximized, which improves the efficiency. The joint reactions can be described by the following simplified relation [27], [31]:

$$\begin{aligned} \mathrm{C}_x\mathrm{H}_y + \left(\frac{1}{2}\,x\,\mathrm{OCR}\right)\mathrm{O}_2 + x\,\mathrm{SCR}\,\mathrm{H}_2\mathrm{O} \\ \longrightarrow x\,\mathrm{CO} + \left(x(2-\mathrm{OCR}) + \frac{1}{2}\,y\right)\mathrm{H}_2 \\ + x\,(\mathrm{OCR} + \mathrm{SCR} - 1)\,\mathrm{H}_2\mathrm{O} \end{aligned} \tag{1}$$

where for diesel fuel x and y equal 14 and 26, respectively, oxygen-to-carbon ratio (OCR) is molar O_2-to-C ratio (typically 0.41–0.47), and steam-to-carbon ratio (SCR) is molar H_2O-to-C ratio (typically 1.7–1.9). Further fuel processing steps (i.e., cleanup) comprise removal of sulphur and CO. Sulphur is trapped in the desulfurizer (DS). Most of the CO is in the presence of water converted into H_2 and CO_2 through the water-gas shift (WGS) reaction

$$\mathrm{CO} + \mathrm{H}_2\mathrm{O} \longleftrightarrow \mathrm{H}_2 + \mathrm{CO}_2. \tag{2}$$

In part, this reaction takes place already in the ATR, but the majority of the conversion occurs in the dedicated WGS reactor [32]. The CO concentration levels in the reformate leaving the reactor are of a few thousand (parts per million) ppm (typically 1000–3000 ppm). The second CO-concerning reaction is the preferential oxidation (PrOx)

$$2\mathrm{CO} + \mathrm{O}_2 \longrightarrow 2\mathrm{CO}_2 \tag{3}$$

taking place in the PrOx reactor with the help of selective catalytic reaction [32]. There, the CO concentration is further decreased down to below 25 ppm. Such a reformate is suitable to be fed to the fuel cell stack without any harmful effects.

For initial preheating, the diesel-powered start burner (SB) is used. From its exhaust, the heat is taken via two air heat exchangers (HEX 1 and 2). For the start of reforming, the steam is generated by another HEX, located at the SB exhaust (not shown in Fig. 2 to avoid excess complexity), before the catalytic afterburner (CAB) operation starts.

In the second *hydrogen-to-electricity* step, typically 70%–80% of the H_2 is converted to electricity within the fuel cell stack. The remaining H_2 is combusted in the CAB [33], and the generated heat is used to prepare superheated steam for the ATR, thus increasing the overall efficiency.

B. APU System

The developed APU system, shown in Fig. 3, has a net electric output power of 3 kW. Its main operational parameters for the tested range with 65% H_2 utilization are summarized in Table I. Beside the fuel processor and the fuel cell stack, it comprises

Fig. 3. Diesel-powered fuel cell APU, comprising the fuel cell module (in front) and fuel processor module (in back).

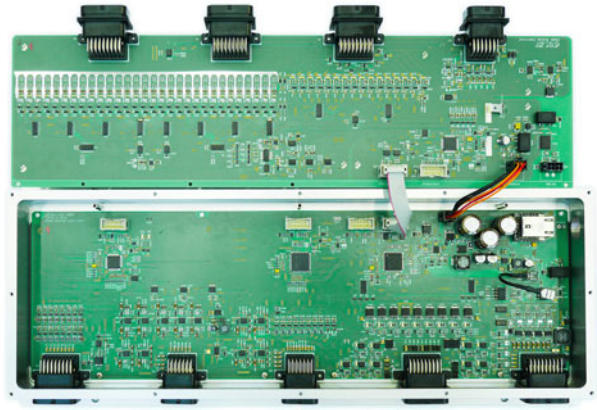

Fig. 4. Electronic control unit composed of two PCBs.

TABLE I
MAIN PARAMETERS OF THE APU

Parameter	At 55% load	At 85% load
Input fuel thermal power	7.0 kW	11.5 kW
Gross electric power[1]	1.83 kW	2.90 kW
Net electric power[2]	1.35 kW	2.10 kW
Gross efficiency[1]	26.1%	25.3%
Net efficiency[2]	19.3%	18.4%
BoP components consumption	420 W	680 W
DC–DC converter losses	50 W	107 W

[1]Electrochemical fuel-to-electricity conversion.
[2]Complete fuel-to-system-output conversion (including dc–dc converter and BoP components).

TABLE II
ELECTRONIC CONTROL UNIT INPUT AND OUTPUT SIGNALS

Signal type		Quantity
Input		
	Standard precision analog inputs (0–25 V)	10
	High precision analog inputs (0–5.5 V)	16
	Mass flow meter inputs	5
	Lambda sensor input	1
	Hall effect current sensor input	1
	Thermocouple inputs with break detection	30
	Pt-1000 resistive temperature sensor inputs	16
	Tacho inputs	8
Output		
	Medium current digital outputs with PWM*	9
	High current digital outputs with PWM	9
	CMOS digital output with PWM capability	8
	Analog outputs (six of them with ground sense capability)	16

*PWM – pulse-width modulation.

numerous BoP components, supporting subsystems and sensors that enable safe and autonomous operation of the overall system.

The BoP components list includes nine valves, 12 pumps, 16 compressors, blowers and fans, 39 temperature sensors, nine mass flow meters, seven pressure sensors, two level sensors, and four gas concentration sensors. For powering all these actuators and sensors, a central power distribution board was built, which is described in more detail in Section IV-B. Moreover, the sensor signals have to be acquired and the actuators have to be controlled. These tasks are served by a tailor-built ECU, shown in Fig. 4.

The ECU has 87 sensor inputs and 48 actuator outputs. The ECU signal channels are listed in Table II. Additionally, it has Ethernet and two controller area network (CAN) communication interfaces. It incorporates four microcontrollers. The main one handles the Ethernet and CAN communication, collects data from and sends data to the supporting processors, and runs the control algorithms. The three supporting processors perform D/A and A/D tasks.

The last important building block of the APU is the direct-current-to-direct-current (dc–dc) converter. It is the connecting block between the fuel cell stack and the electric power system of the vehicle. The output voltage of the stack varies between 33 and 47 V, whereas the nominal voltage of the vehicle electric power system is 24 V. Therefore, a step-down dc–dc converter is mounted in between the stack and the electric power system of the vehicle, as shown in Fig. 1. The dc–dc converter and its protection functionalities are described in Section IV-A.

III. MITIGATION CONTROL STRATEGIES

The APU system is affected by various phenomena reducing its reliability and life-time. To counter these, the control system has to be able to drive the APU process away from the boundary conditions, while also optimizing its efficiency. There are three factors making the control task challenging:

1) the APU process nature, defined by a number of downstream-connected chemical reactors;
2) the reactors' intolerance to impurities; and
3) diesel as the input fuel, which, compared to LPG or CNG, is more difficult to handle [3].

These impose two requirements: 1) each reactor must operate within its strict operation parameter values, and 2) the reformate stream leaving one reactor must be of adequate quality (gas concentrations and temperature) to safely enter the next one. The required reformate stream quality in terms of gas concentrations, tolerated impurities, and temperatures is presented in Fig. 5. A control system failing in fulfilling its assigned tasks results in the following:

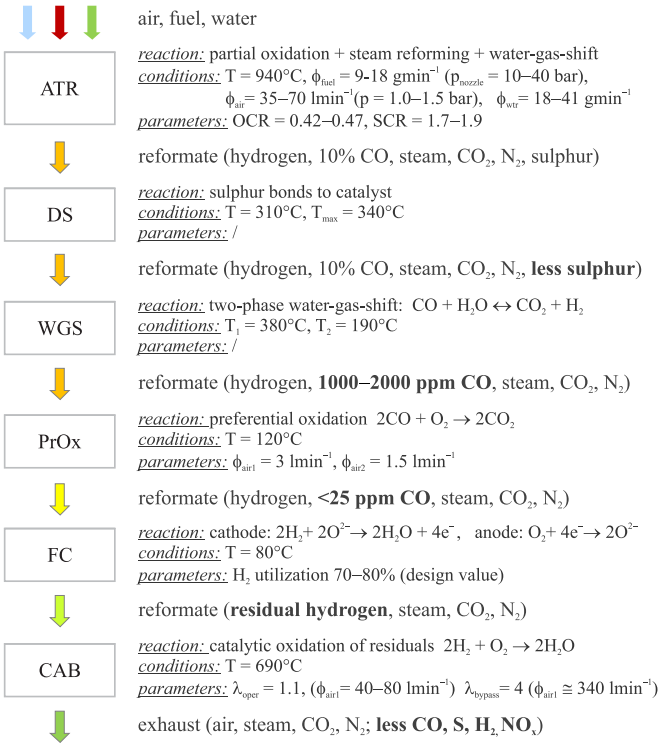

Fig. 5. Fuel conversion path with all reactors, their residing reactions, operating parameters, and reformate gas contents.

1) suboptimal diesel conversion (any impurity or other disturbance propagating from the preceding reactor down to the following ones);
2) carbonaceous substance deposition onto the catalyst;
3) damage or deactivation of the catalyst; and
4) damage of the fuel cell stack.

In the following, the most common harmful phenomena are described and a description of control means for avoiding and mitigating them are given.

A. System-Threatening Phenomena

1) CO Poisoning: Low-temperature PEM fuel cells are prone to CO poisoning [34]–[36]. CO concentrations exceeding 25 ppm result in a bonding of the molecules to the Pt catalyst structure. This reduces its active area, making the reaction less efficient. The CO poisoning is reversible to a degree. The APU system has an air-bleed function [37], oxidizing CO to CO_2, to suppress its effect in case of possible suboptimal reformate quality. The downside of this approach, in the case of constant excessive CO content, is a high impact on the efficiency [38].

PrOx reactor temperature needs to be within a narrow temperature range in order to guarantee catalyst selectivity and maintain the required CO levels. This is especially challenging during load transients. If the temperature goes outside the range, the PrOx reactor starts oxidizing more H_2 instead of CO. As a result, the CO level peaks and poisons the fuel cell stack.

2) Diesel Poisoning: Long-chain hydro-carbon molecules, composing diesel fuel, have a high boiling point (~250–350 °C) and are therefore likely to deposit on the reactor catalysts of lower temperatures [39], [40]. Within the APU, several reactors are prone to this kind of poisoning. These include WGS, PrOx, and the fuel cell stack, as at least parts of them never reach temperatures that high.

3) Water Condensation: Liquid water on the catalyst may present danger in certain conditions. The danger of damage occurs in the case of fast temperature rise (e.g., reaction start) [39]. Then, the water evaporates and its volume increases instantly and significantly. Such an explosion inside of a porous catalyst structure damages the structure and the catalyst active area. Water condensation has therefore to be avoided in reactors, where the start of reaction suddenly increases the temperature. To prevent it during the startup procedure, the reactors have to be heated above their dew points before starting the reaction. Whereas during shutdown, the water has to be completely removed from the reactors before cooling them down completely.

4) Soot Ignition: During operation in suboptimal conditions, but predominantly during startup and shutdown procedures, soot may be produced and deposited on downstream reactors. In the case of exceeded soot-ignition temperature (300–400 °C) [41], and in the presence of air, the deposited soot may ignite, resulting in very high temperature and pressure, damaging the reactor.

The reactor most prone to this phenomenon is the DS unit, i.e., the sulphur trap. The ignition may occur during the shutdown procedure. In an attempt to cool the ATR reactor down and remove water from it, air is passed through the hot ATR reactor, where it heats up to 500 °C and then enters the DS unit. Due to the hot air present, the soot in the DS unit can ignite, resulting in temperature spikes up to 800 °C, damaging the reactor. Moreover, if the DS unit is heated above 350 °C, it releases all of the accumulated sulphur downstream, damaging downstream reactors. Similarly, the ATR reactor itself is also prone to soot ignition, where the soot may ignite during startup heating, when hot air is present in excess.

5) Overheating: All of the discussed reactors are sensitive to overheating. In some cases, the residing reaction may be the cause, while in others, it is the reformate coming from the upstream reactor. The overheating is emphasized by stiff, high-order process dynamics that may lead to uncontrollable conditions if not handled well. The overheating issues are listed in Table III.

6) Nozzle Clogging and Reduced Spray Quality: The ATR operation requires the fuel to be dispersed before the reforming starts, thus accelerating evaporation and increasing the fuel conversion to near 100%. This is achieved by spraying the fuel with very high pressure through a fine nozzle. Due to high temperatures and sedimentation (predominantly during startup and shutdown), the heavy fractions may form deposits on the inner surface of the nozzle if not treated properly. The depositions reduce the diameter of the nozzle aperture. As a result, the spray quality gradually deteriorates (lesser conversion quality), and finally transforms into a jet, destroying the ATR's catalyst at the place of impact.

7) Reactant Starvation in Fuel Cell: This threat exists due to the significant difference in the dynamics of the electrical

TABLE III
APU'S REACTORS OVERHEATING CAUSES

Component	Overheating cause
ATR	Partial/full oxidation—a small increase in air flow or reduction in fuel flow has a major immediate effect on catalyst temperature increase.
DS	Strong ATR air-cooling with or without soot ignition, slow & weak cooling structure.
PrOx	Change of reaction front in various operating points together with slow or uninformative sensor response, slow cooling effect due to large reactor mass.
CAB	In certain operation modes, a small decrease in air flow or increase in H_2 content (caused by changed load) has a substantial immediate effect to catalyst temperature spike.
HEX 1 and 2	After SB operation stops, its cooling brings significant heat to the SB HEX1 and 2, and may damage them.

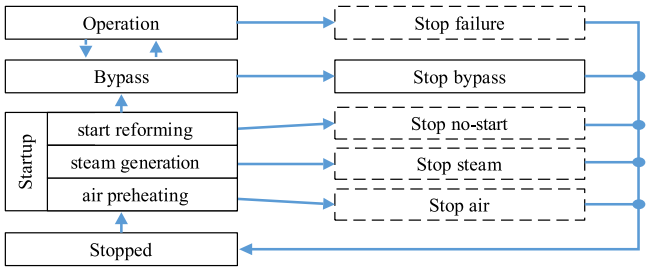

Fig. 6. APU operation state transition diagram. Regular operation modes (solid line) and emergency modes (dashed line).

and chemical parts of the system. On the electric side, a load switch is instantaneous, while the fuel processor requires up to 30 s to reach the required operating point upon load change. A sudden increase in electric load demand may therefore result in fuel cell gas starvation, as there is not sufficient reformate available.

B. Condition-Aware Control Strategies

The fuel reforming process and its operation equilibria have been defined and verified through simulation and experimentation [42]. There, the process operating points have been identified and operation ranges for various parameters specified. Having that data, the function of control is threefold:

1) to bring the system to the operating points;
2) to maintain the operation within the specified range; and
3) to safely stop it.

The control is managed by a high-level supervisory sequential controller in the form of a state machine shown in Fig. 6. The states have procedures and functions tailored to ensure system response in accordance with the current operating conditions and regime. Typical examples of such control are startup and shutdown procedures, where the actuators are started, stopped, or controlled one by one, using ramps and timers.

1) Startup Procedure: The fuel processor is first heated up by hot air via two channels. The first goes through the ATR, DS, WGS, and PrOx reactors, and the second heats up the CAB. The heating air, reaching approximately 600 °C, is heated by HEXs within the start-burner exhaust. The ATR has to reach above 350 °C, while other reactors have to be heated above the dew point to approximately 75 °C to prevent water condensation. The challenge arises from the significant thermal mass of the reactors and the upper temperature limit of 350 °C imposed by the DS unit. The temperature rise is fast in the ATR and DS, but very slow in the PrOx. This results in the DS reaching its upper limit much earlier than the PrOx reaches its target temperature. To prevent the DS from overheating, half of the air is diverted to pass the HEX1 and goes directly to the ATR (normal operation path) until the DS temperature starts dropping.

After the preheating stage, the most critical startup phase follows. The fuel enters the system; the thermal load jumps from zero to ca., 6 kW in seconds; and, the temperatures peak from 300 to 900 °C and from 150 to 700 °C in the ATR and CAB reactors, respectively. More precisely, the reforming and related temperature control loop for the ATR reactor start first. Moments later, the prepared reformate, bypassing the fuel cell stack, enters the CAB, starting the catalytic combustion. The control of both reactors is described in Section III-C.

The maximal values for sulphur, diesel slip (non-methane-hydro-carbons), and CO tolerated by PEM fuel cells are extremely low (10 ppb, 1 and 25 ppm, respectively). However, for the reactions to take place in full range enabling production of reformate with adequate quality, the reactors have to reach the predefined narrow temperature ranges. While waiting for the temperatures to settle, the generated reformate needs to be combusted to fully comply with allowed exhaust regulations (NO_x, CO, temperature, etc.) and not to release explosive hydrogen to the environment. To cope with that, the reformer system employs a bypass mode, where the reformate gas completely bypasses the fuel cell stack and is burned in the CAB.

The startup procedure may proceed to the bypass and further to operation mode or any of the shutdown procedures depending on the cause and the active phase of the startup, as can be seen in Fig. 6.

2) Shutdown Procedures: To ensure reliable APU operation and multiple starts, the task of the shutdown procedure is to safely stop the process from any possible operation state and prepare the system for the new start. For guaranteed robustness, the shutdown procedure is a sequence of actions that use as few sensors and feedback control loops as possible, as it must operate reliably also in the case of sensor failures. In general, the shutdown has three main functions that take place in the following sequence:

1) cooling of reactors to safe temperatures and prevention from overheating downstream components;
2) purging reactors with steam to push out all remaining hydro-carbons or other potential deposition-forming substances; and
3) purging reactors with air to remove all water and prevent condensation.

Considering various combinations of reactants present in the reactors in different operation modes, in total five shutdown procedures have been developed, as shown in Fig. 6.

1) Regular shutdown: The termination of the reforming reaction often results in short-term increased diesel and CO concentrations. To prevent them from entering the fuel cell stack, the system is first put to the *bypass mode*.

However, the CAB can only handle complete reformate flow at half load. Therefore, to prevent the CAB reactor from overheating, the load is first decreased to its lowest operating point, then the bypass mode is introduced, and only then is the reforming terminated and cooling starts. While cooling, it is important not to push the heat downstream toward the temperature-sensible reactors (i.e., DS, PrOx). To counter that, the DS precooling phase is introduced to the shutdown procedure after experiencing ignition of soot decompositions due to excessive temperature and the presence of air.

2) Emergency shutdown procedures:

a) Stop-no-start: With degraded catalyst, or insufficient startup heating power, the ATR reaction may not start when fuel is injected. Then, the system must be stopped and purged properly. Compared to normal procedure in the *no-start case*, the water cooling phase must take longer. To prevent the ignition of fuel, which accumulated in the ATR during the unsuccessful start, air cooling has to be introduced gradually before decreasing the water flow. Consequently, the air-purge stage is prolonged to ensure removal of all water from the system and avoid condensation.

b) Other emergency procedures: The emergency stopping procedures are prepared for three stages of process content:

1) air preheating—in this case, only air is present in the reactors, and only little air cooling is required;
2) steam generation—water presence in the system requires air-purging to prevent water condensation;
3) reforming—fuel in the system requires steam purging, an anti- "nozzle clogging" procedure, and air-purging.

An example of an event requiring an emergency stop is the system running out of water while reforming. Without an immediate action, the ATR catalyst overheats and terminally deactivates. A similar effect can have a failure of any reactant-supplying BoP component due to overheating or ageing.

C. Use of Advanced Means in Operational Control

The complexity and the high degree of interaction of the reforming process, amplified by a high number of sensors and actuators, requires a combination of top-down and bottom-up approaches to form a robust control system. To improve the operation quality and reliability, several techniques have been employed.

1) Load Control: The reactor process dynamics is governed by the residing chemical reaction and the reactor structure. Most reactors of the described system have stiff dynamics: the fast-responding catalytic reaction, and significant slow-responding housing temperature dynamics. In many cases, a slow controller is required to suppress noise disturbances, and at the same time a fast response to operating point change is necessary to prevent harmful temperature peaks. Furthermore, with different operating points (loads), the reaction front (i.e., the position of the reaction) in a reactor changes. This affects the response dynamics of the sensors and leads to temperature instability. Therefore, the operating points of most reactors are set by the feed-forward control based on reformer load, and the feedback control takes care for precise set-point tracking and disturbance rejection.

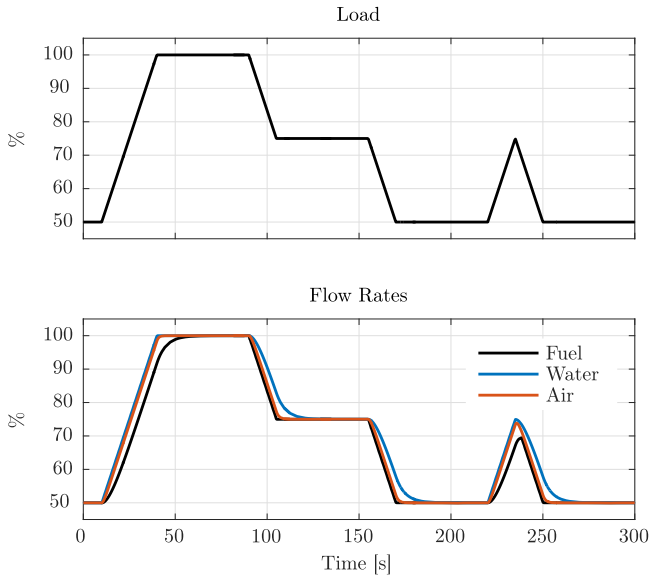

Fig. 7. Dynamic relation between flow rates (fuel, water, air).

2) Switching Dynamics Control: To guarantee nominal conditions and to prevent fluctuations in reactor temperature and reformate concentrations during operating point change, the ramp-shaped transitions are used. Furthermore, to enable faster transitions while still ensuring safe operation, the double-dynamic first-order [low-pass, (LP)] filters have been applied to the set-points for reactants flows, namely for fuel, air, and water. Each LP filter is determined by two time constants, one is active when the input signal increases, the other is active when the input signal decreases. In such a way, filtered reactant set-points are shown in Fig. 7. Note the different increasing/decreasing dynamics for certain flow set-points.

3) ATR Operation Control: As described before, three input reactants are required for autothermal reforming, namely, air, fuel, and steam. Air and fuel flows are provided to the ATR directly by a blower and a high-pressure pump, respectively. The water is fed through the CAB, where it is evaporated. Within the ATR, the exothermic partial oxidation and the endothermic steam reforming compete. The heat released by the partial oxidation maintains the reactor at the temperature enabling the steam reforming.

Ensuring complete diesel conversion and preventing the so-called diesel slip requires maintaining the temperature as high as possible, but not above 950 °C, regardless of the thermal load (to prevent degradation). This is not straightforward, as the absolute thermal losses (through insulation) remain the same, while the reaction energy increases with the operating point. Therefore, at higher loads, relatively less energy is required for maintaining the endothermic reforming. Consequently, the operation parameters need to be changed. In general, the ATR catalyst temperature could be controlled by accommodating the air-flow rate to the ATR. By increasing the air-flow rate, a greater

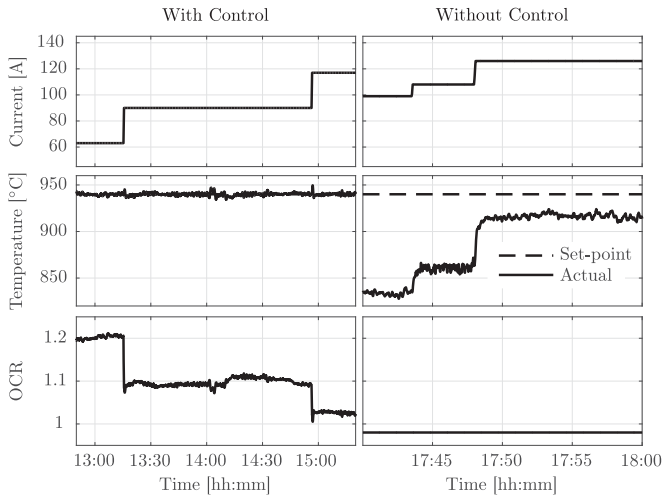

Fig. 8. ATR catalyst temperature response to ATR load change with (left) and without (right) control. Signals: fuel processor load (top), ATR temperature (middle), and ATR OCR ratio (bottom).

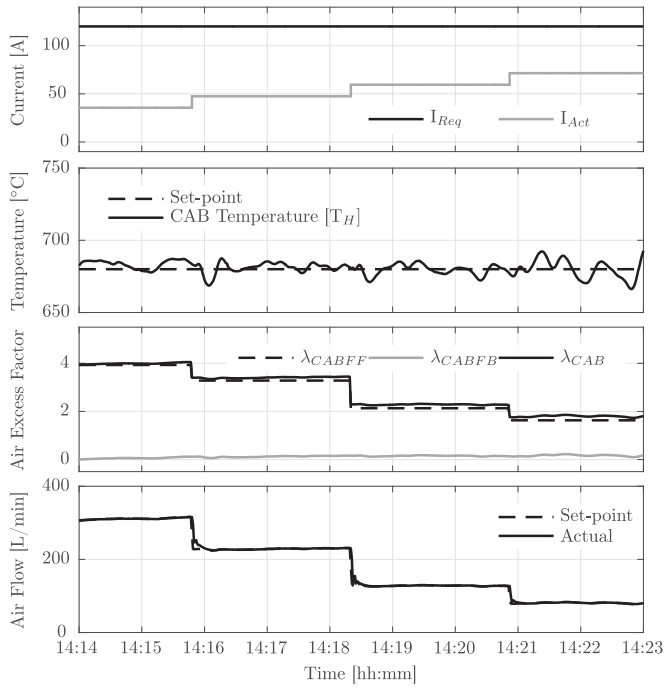

Fig. 9. CAB reaction temperature control in the presence of fuel cell current change as disturbance, with constant fuel processor load. The charts present fuel processor and fuel cell load (top chart), CAB temperature (second chart), λ factors (third chart), and CAB air flows (bottom chart).

part of the fuel is oxidized, and consequently the heating power and temperature increase. However, by changing only the air-flow rate and not accommodating for fuel and water-flow rates, the flow rate of produced hydrogen changes, which is not acceptable from the point of fuel cell operation. In [27], it was shown that the catalyst temperature can be controlled by changing the OCR instead of the air-flow rate directly. This way the temperature control can be decoupled to have no influence on the flow rate of produced hydrogen. To obtain the best possible control over the ATR catalyst temperature for all operating points as well as during the load change, the OCR is defined as a combination of nominal value, lookup table addition, and temperature controller

$$\mathrm{OCR} = \mathrm{OCR_{Nom}} + \mathrm{OCR_{Map}} + \mathrm{OCR_{Cl}} \tag{4}$$

where $\mathrm{OCR_{Nom}}$ is the nominal OCR value, $\mathrm{OCR_{Map}}$ is the mapped correction based on the reformer load, and $\mathrm{OCR_{Cl}}$ is the ATR-temperature controller correction, enabling precise temperature tracking. The examples of controlled and noncontrolled ATR temperature response to load change are shown in the left and right charts of Fig. 8, respectively.

4) CAB Temperature Control: The catalytic afterburner reactor is used to burn combustible content in reformate before leaving gases into exhaust. In the presented configuration, it serves two purposes and operates in two significantly different regimes. Most of the time, in operation mode, it is used to burn the residual H_2 in the fuel cell anode off-gas and, using the generated heat, prepares steam for the ATR. In this operation mode, the air is supplied with a stoichiometric ratio (λ) slightly above 1.0, i.e., just sufficient to burn combustible contents. The other regime is used in the bypass mode, where the total amount of generated reformate is combusted. In this case, the air is supplied at $\lambda \approx 4$. In this regime, the water flow is not sufficient for cooling. Therefore, a large surplus of air is added for additional cooling.

The challenge originates from momentary events, such as switching between operation and bypass, or even more difficult, when a large electric load is (dis)connected. The switching from/to bypass is normally a deliberate event, and the blower supplying air is given a "heads-up" to prepare sufficient flow. On the other hand, in the case of fuel cell load change, the stack current value is the fastest indication of altered conditions. To cope with this, several feed-forward inputs are used for the CAB air-flow set-point [28]: the reformer load, the stack current, and the desired λ (depending on operating mode). They define the estimated H_2 flow to CAB and λ_{FF}. Finally, the temperature controller adds the feedback corrected λ_{FB}

$$\phi_{\mathrm{CAB_{air}}} = 0.5/0.21\, \phi_{\mathrm{CAB}_{H2est}} (\lambda_{FF} + \lambda_{FB}) \tag{5}$$

where 0.21 is the air O_2 content, 0.5 is the molar oxygen-to-hydrogen ratio in H_2O, the $\phi_{\mathrm{CAB}_{H2est}}$ is the model-estimated H_2 flow coming out of the stack, λ_{FF} is the mapped feedforward, and λ_{FB} the feedback defined value of the stoichiometric ratio λ. This way the air flow is guaranteed to have a fast and precise response. Thus, the temperature spikes are effectively reduced. An example of effective temperature control in the presence of fuel cell current variation is shown in Fig. 9.

5) Cooling Loops: The cleanup reactors require cooling, which is provided by water pumps for DS and PrOx, and an air blower for WGS. The cooling loops were tuned predominantly to maintain the output reformate CO concentration below the required 25 ppm at all times. Since small integrable CO sensors do not exist, the CO concentration was measured only during

tuning using Fourier transform infrared spectroscopy, to define the precise temperature operating ranges of the reactors.

From the control aspect, there are two challenges: 1) the reactor structures impose high-order dynamics, often combined with long lag times, and 2) the reaction (catalyst) temperature measurements are very noisy due to turbulent reactions. Therefore, to achieve quality control, the cooling loops require a slow response. However, this is not beneficial for successful compensation of load set-point changes that require a fast response. To counter that, a feedforward extended proportional-integral-derivative (PID) controller [43] is used

$$u = k_{ff}\, I_{\text{load}} + k_p \text{Err} + \frac{k_p}{\tau_i}\int \text{Err}\, dt + k_p T_d \frac{dErr}{dt} \qquad (6)$$

where I_{load} defines the process operating point and k_{ff} is the experimentally tuned feedforward gain, and the rest are general PID controller parameters. If required, the feedforward signal may be treated also with a lookup table to achieve the desired response.

IV. Power Electronic Hardware Solutions for Ensuring Reliable and Durable Operation

Electronic components that were specifically designed for the APU system include a step-down dc–dc converter, a power distribution board, and an ECU. Preventing possible operation faults and ensuring smooth operation were the main guidelines during the development of the components. The ECU is described in Section II-B and shown in Fig. 4, whereas the dc–dc converter and the power distribution board and their protection functionalities are presented in the following.

A. DC–DC Converter

In systems with fuel cells, a dc–dc converter is required for power conditioning [44]–[48]. It connects the stack to the electric power system of the vehicle. Its main function is to adjust the varying (nonregulated) output voltage of the fuel cell stack to the voltage level of the vehicle's power system. In addition, it is an essential building block of the power management system, providing the means for efficient power management of the APU-battery-vehicle-user arrangement.

The output voltage of the APU fuel cell stack depends on the load current varying between 33 and 47 V. The electrical power system of the vehicle has a nominal operation voltage of 24 V and is predominantly defined by the main lead-acid battery, whose voltage ranges from 21 to 28.8 V. As a result of these constraints, the dc–dc converter is designed based on a step-down (buck) topology. The step-down power stage is controlled by an embedded microcontroller. The microcontroller provides the set-point for the current through its D/A converter. Yet, the power stage is designed as a self-sufficient block, which needs no microcontroller intervention to oscillate and to control the output current. Consequently, the safety of the power conversion control is not affected by any software errors or strong external transients, which may cause the microcontroller to operate temporally in an undefined state.

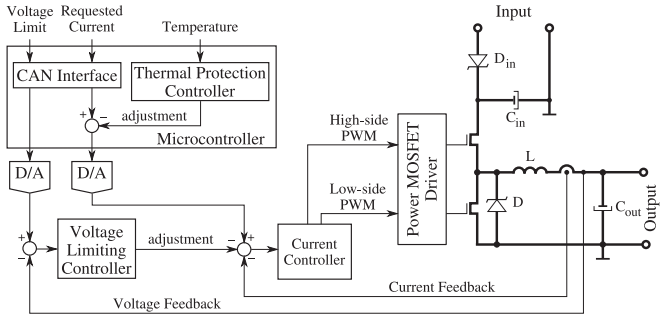

Fig. 10. Control scheme of the dc–dc converter.

The dc–dc converter built for the APU is an enhanced version of the dc–dc converter presented in [23]. Among others, the enhancements concern *thermal protection and voltage limiting capabilities*, which add to the reliability of the overall APU system. The control of the converter is designed such that the output (inductor) current is under primary control (the inner control loop from the scheme is provided in Fig. 10). Therefore, the only way to affect the operation of the converter is through adjustment of the set-point for the inner control loop. In this manner, both of the protection functionalities are designed. The request for the amount of output current is sent to the converter's microcontroller via the CAN interface. If there are no damaging conditions (i.e., too high temperature or output voltage), the request is transferred unchanged to the inner control loop. Otherwise, the current set-point for the control loop is adjusted (decreased) by the corresponding thermal protection or voltage limiting controller.

The power metal-oxide-semiconductor field-effect transistor (MOSFET) of the converter are exposed to substantial thermal stress. In order to prevent the MOSFET from deterioration and failures, their temperature is supervised by the microcontroller. The microcontroller acquires the temperature over a negative temperature coefficient thermistor and adjusts (i.e., decreases) the electric current set-point if the temperature is above the temperature threshold. The set-point lowering strategy is implemented as a proportional-integral control algorithm.

Since the dc–dc converter is installed between the fuel cell stack and the vehicle's battery, its output voltage is determined by the battery's voltage. In order to protect the battery from overcharging and overvoltage, the dc–dc converter has to be able to limit the output voltage. This is the task of the voltage limiting controller. Similar to the thermal protection, the voltage limiting controller steps-in only when the voltage reaches the preset limit (the limit is passed to the converter's microcontroller via the CAN interface). Essentially, the output voltage is limited by decreasing the electric current set-point signal for further dc–dc control circuitry (i.e., inner current control loop). A simplified scheme of dc–dc converter control loops is shown in Fig. 10.

Since the converter's current is under primary control, the voltage (limiting) control steps-in only when the voltage reaches the preset limit. Essentially, the voltage is limited by affecting the electric current reference signal for further dc–dc control circuitry. A scheme of the dc–dc converter control loops is shown in Fig. 10.

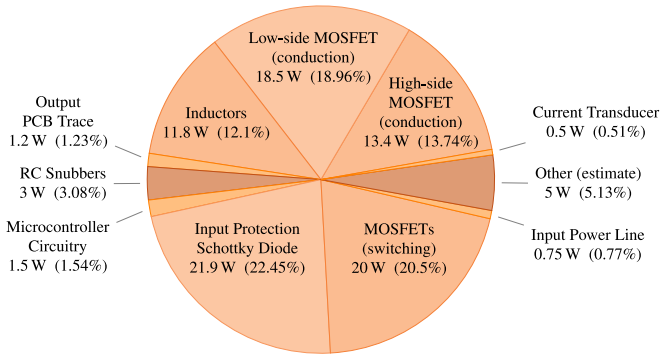

Fig. 11. Power-loss breakdown of the dc–dc converter measured at input power of 2027 W.

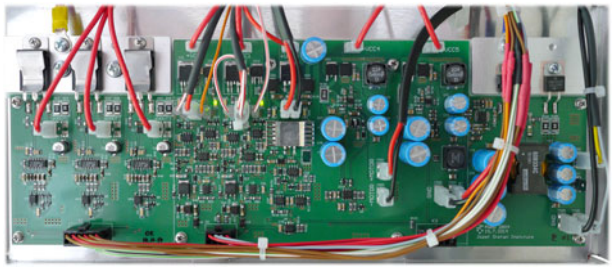

Fig. 12. Power distribution board.

The efficiency of the dc–dc converter varies with current and voltage and is no less than 95%. Measurements of power losses on individual components obtained at a load of 2027 W are given in Fig. 11. As can be seen in the pie chart, the losses that increases as the square of the current account for approximately one half of all losses, meaning higher efficiency at a lower current. Moreover, the 95% efficiency accounts as well for the losses of the input protection Schottky diode that prevents the current from flowing into the fuel cell stack. This would occur in case of unpredictable circumstances when the voltage at the output of the converter would be higher than the fuel cell stack's voltage.

B. Power Distribution

Power demand is ever increasing in vehicular power systems, hence more sophisticated power distribution infrastructure is favored [49]. As explained in Section II, the APU comprises a vast number of sensors and actuators of various types. The electronics of these devices require a variety of power supply types (different voltage levels, pulse-width modulation (PWM) operation, etc.) Moreover, they have to be protected against possible electrical disturbances. In order to keep costs low, the power distribution was designed in a centralized manner as a compact board (as shown in Fig. 12).

The board provides a power supply with *overvoltage protection* for powering the sensitive electronics of the lambda sensor, mass flow meters, level sensors, etc. The power supply is designed as a step-down dc–dc converter based on Texas Instruments LM5085 switching controller. The switching controller provides instantaneous overvoltage protection of the output. Thus, the possibility of malfunction of the powered sensor is substantially reduced. Furthermore, the design can operate at 100% duty cycle resulting in a low dropout voltage, which is especially convenient in case of an unpredicted drop in the supply voltage below the intended output voltage. In this case, the output remains active with a voltage of just a few millivolt below the input voltage.

The APU consists of a high number of sensors and actuators. When these components are connected to the vehicle power supply, their input capacitors have to be charged resulting in a very high inrush current. This current would have an undesired effect on the main battery and other electronic parts of the vehicle. To avoid high *inrush current*, the power distribution board encompasses precharge circuitry. In its essence the precharge circuitry limits the charging current by passing it through a power resistor. When the voltage settles, the resistor is bypassed by a relay thus eliminating the power resistor losses during normal operation.

When the vehicle battery is unintentionally disconnected (e.g., loose terminal clamp at the battery together with vibrations), the alternator temporarily raises up the system voltage. This effect is known as load dump [50], [51]. According to the ISO 16750-2:2010(E) Standard, for 24-V vehicle power systems, the voltage may raise up to 202 V for a few hundred milliseconds [52]. However, in modern trucks, a centralized load dump suppression is implemented as a part of the alternator's rectifier (i.e., Zener transient voltage suppressor). When such a suppressor is present, the voltage surge is limited to 65 V. Since the APU power system is connected to the vehicle's power system, the *load dump protection* for it is necessary and is implemented as a part of the power distribution board.

The power distribution board has three separated load dump protection channels. The protection is designed using a Liner Technology LT4363 surge stopper and a power MOSFET. The circuitry protects against input voltage surge in accordance with the ISO 16750-2:2010(E) Standard and against overcurrent. When a voltage surge occurs at the input, or the current is above the threshold, the gate of the MOSFET is controlled in order to regulate the output voltage. The excess energy is dissipated as heat on the MOSFET, thus the output voltage remains within the tolerable levels.

V. Conclusion

Control strategies and electronic hardware solutions for increasing the reliability and extending the life-time of a diesel-powered fuel cell APU system were presented in this paper. The two main modules of the system were an ATR-based diesel reformer and a PEM fuel cell stack. The harmful phenomena affecting the reliability of the APU were described, and the corresponding mitigation control strategies were thoroughly discussed. In addition, the developed electric hardware modules with protection functionalities were presented. The effectiveness of the proposed solutions was shown on validation data obtained on a 3-kW net electric power APU system, primarily designed for truck on-board applications.

ACKNOWLEDGMENT

The research and development activities leading to these results have been carried out within the http://www.fcgen.com EU FP7 FCGEN project. The authors would like to thank the contribution of the FCGEN project consortium partners: Volvo Technology, PowerCell, FZH Jülich, Fraunhofer ICT-IMM, Johnson Matthey, and Modelon, and thank them for sharing their valuable experience and knowledge.

REFERENCES

[1] L. Valverde, C. Bordons, and F. Rosa, "Integration of fuel cell technologies in renewable-energy-based microgrids optimizing operational costs and durability," *IEEE Trans. Ind. Electron.*, vol. 63, no. 1, pp. 167–177, Jan. 2016.

[2] O. Z. Sharaf and M. F. Orhan, "An overview of fuel cell technology: Fundamentals and applications," *Renewable Sustain. Energy Rev.*, vol. 32, pp. 810–853, 2014.

[3] G. Kolb, "Review: Microstructured reactors for distributed and renewable production of fuels and electrical energy," *Chem. Eng. Process.*, vol. 65, pp. 1–44, 2013.

[4] J. D. Rojas, C. Kunusch, C. Ocampo-Martinez, and V. Puig, "Control-oriented thermal modeling methodology for water-cooled PEM fuel-cell-based systems," *IEEE Trans. Ind. Electron.*, vol. 62, no. 8, pp. 5146–5154, Aug. 2015.

[5] P. Engelhardt, M. Maximini, F. Beckmann, M. Brenner, and O. Moritz, "Coupled operation of a diesel steam reformer and an LT- and HT-PEFC," *Int. J. Hydrogen Energy*, vol. 39, no. 31, pp. 18 146–18 153, 2014.

[6] B. Lindström *et al.*, "Diesel fuel reformer for automotive fuel cell applications," *Int. J. Hydrogen Energy*, vol. 34 , no. 8, pp. 3367–3381, 2009.

[7] R. C. Samsun, J. Pasel, R. Peters, and D. Stolten, "Fuel cell systems with reforming of petroleum-based and synthetic-based diesel and kerosene fuels for APU applications," *Int. J. Hydrogen Energy*, vol. 40, no. 19, pp. 6405–6421, 2015.

[8] "DESTA project to demonstrate european SOFC truck APU," *Fuel Cells Bull.*, vol. 2012, no. 5, p. 4, 2012.

[9] "PURE (development of auxiliary power unit for recreational yachts)." 2013. [Online]. Available: http://www.fch.europa.eu/project/development-auxiliary-power-unit-recreational-yachts

[10] "FCGEN (fuel cell based power generation)." 2011. [Online]. Available: http://www.fch.europa.eu/project/fuel-cell-based-power-generation

[11] "Diesel-powered fuel cell produces clean electricity." Jul. 17, 2015, [Online]. Available: http://spectrum.ieee.org/energywise/energy/fossil-fuels/dieselpowered-fuel-cell-produces-green-electricity

[12] D. Krekel, R. C. Samsun, J. Pasel, M. Prawitz, R. Peters, and D. Stolten, "Operating strategies for fuel processing systems with a focus on water-gas shift reactor stability," *Appl. Energy*, vol. 164, pp. 540–552, 2016.

[13] S. J. Andreasen, S. K. Kær, and S. Sahlin, "Control and experimental characterization of a methanol reformer for a 350 W high temperature polymer electrolyte membrane fuel cell system," *Int. J. Hydrogen Energy*, vol. 38, no. 3, pp. 1676–1684, 2013.

[14] R. C. Samsun, C. Krupp, A. Tschauder, R. Peters, and D. Stolten, "Electrical start-up for diesel fuel processing in a fuel-cell-based auxiliary power unit," *J. Power Sources*, vol. 302, pp. 315–323, 2016.

[15] M. Maximini, P. Engelhardt, M. Brenner, F. Beckmann, and O. Moritz, "Fast start-up of a diesel fuel processor for PEM fuel cells," *Int. J. Hydrogen Energy*, vol. 39, no. 31, pp. 18 154–18 163, 2014.

[16] D. Vrečko *et al.*, "Feedforward-feedback control of a SOFC power system: A simulation study," *ECS Trans.*, vol. 68, no. 1, pp. 3151–3163, 2015.

[17] H. Ji, J. Bae, S. Cho, and I. Kang, "Start-up strategy and operational tests of gasoline fuel processor for auxiliary power unit," *Int. J. Hydrogen Energy*, vol. 40, no. 11, pp. 4101–4110, 2015.

[18] L. Nieto Degliuomini, D. Zumoffen, and M. Basualdo, "Plant-wide control design for fuel processor system with PEMFC," *Int. J. Hydrogen Energy*, vol. 37, no. 19, pp. 14 801–14 811, 2012.

[19] Y. Shen, D. Li, and W. Tan, "Active disturbance rejection control for fuel processing system of fuel cells," in *Proc. 34th Chin. Control Conf.*, 2015, pp. 187–192.

[20] B. Kalmula and V. R. Kondapuram, "Fuel processor—fuel cell integration: Systemic issues and challenges," *Renew. Sustain. Energy Rev.*, vol. 45, pp. 409–418, 2015.

[21] G. Dolanc *et al.*, "A miniature fuel reformer system for portable power sources," *J. Power Sources*, vol. 271, pp. 392–400, 2014.

[22] A. Debenjak, P. Boškoski, B. Musizza, J. Petrovčič, and Đ. Juričić, "Fast measurement of proton exchange membrane fuel cell impedance based on pseudo-random binary sequence perturbation signals and continuous wavelet transform," *J. Power Sources*, vol. 254, pp. 112–118, 2014.

[23] A. Debenjak, J. Petrovčič, P. Boškoski, B. Musizza, and Đ. Juričić, "Fuel cell condition monitoring system based on interconnected DC–DC converter and voltage monitor," *IEEE Trans. Ind. Electron.*, vol. 62, no. 8, pp. 5293–5305, Aug. 2015.

[24] B. Mileva Boshkoska, P. Boškoski, A. Debenjak, and Đ. Juričić, "Dependence among complex random variables as a fuel cell condition indicator," *J. Power Sources*, vol. 284, pp. 566–573, 2015.

[25] B. Dolenc, D. Vrečko, Đ. Juričić, A. Pohjoranta, and C. Pianese, "Online estimation of internal stack temperatures in solid oxide fuel cell power generating units," *J. Power Sources*, vol. 336, pp. 251–260, 2016.

[26] M. Nerat and Đ. Juričić, "A comprehensive 3-D modeling of a single planar solid oxide fuel cell," *Int. J. Hydrogen Energy*, vol. 41, no. 5, pp. 3613–3627, 2016.

[27] G. Dolanc, B. Pregelj, J. Petrovčič, J. Pasel, and G. Kolb, "Control of autothermal reforming reactor of diesel fuel," *J. Power Sources*, vol. 313, pp. 223–232, 2016.

[28] G. Dolanc, B. Pregelj, J. Petrovčič, and R. C. Samsun, "Control of an afterburner in a diesel fuel cell power unit under variable load," *J. Power Sources*, vol. 338, pp. 117–128, 2017.

[29] B. Pregelj, D. Vrečko, J. Petrovčič, V. Jovan, and G. Dolanc, "A model-based approach to battery selection for truck onboard fuel cell-based APU in an anti-idling application," *Appl. Energy*, vol. 137, pp. 64–76, 2015.

[30] B. Pregelj, M. Micor, G. Dolanc, J. Petrovčič, and V. Jovan, "Impact of fuel cell and battery size to overall system performance—A diesel fuel-cell APU case study," *Appl. Energ.*, vol. 182, pp. 365–375, 2016.

[31] J. Pasel, R. C. Samsun, A. Tschauder, R. Peters, and D. Stolten, "A novel reactor type for autothermal reforming of diesel fuel and kerosene," *Appl. Energy*, vol. 150, pp. 176–184, 2015.

[32] M. O'Connell *et al.*, "The development and evaluation of microstructured reactors for the water gas shift and preferential oxidation reactions in the 5 kW range," *Int. J. Hydrogen Energy*, vol. 35, no. 6, pp. 2317–2327, 2010.

[33] R. C. Samsun, J. Pasel, H. Janßen, W. Lehnert, R. Peters, and D. Stolten, "Design and test of a 5 kWe high-temperature polymer electrolyte fuel cell system operated with diesel and kerosene," *Appl. Energy*, vol. 114, pp. 238–249, 2014.

[34] J. J. Baschuk and X. Li, "Carbon monoxide poisoning of proton exchange membrane fuel cells," *Int. J. Energy Res.*, vol. 25, no. 8, pp. 695–713, 2001.

[35] J. J. Baschuk and X. Li, "Modelling CO poisoning and O_2 bleeding in a PEM fuel cell anode," *Int. J. Energy Res.*, vol. 27, no. 12, pp. 1095–1116, 2003.

[36] C. Farrell, C. Gardner, and M. Ternan, "Experimental and modelling studies of CO poisoning in PEM fuel cells," *J. Power Sources*, vol. 171, no. 2, pp. 282–293, 2007.

[37] S. Gottesfeld and J. Pafford, "A new approach to the problem of carbon monoxide poisoning in fuel cells operating at low temperatures," *J. Electrochem. Soc.*, vol. 135, no. 10, pp. 2651–2652, 1988.

[38] J. Tjønnås, F. Zenith, I. J. Halvorsen, M. Klages, and J. Scholta, "Control of reversible degradation mechanisms in fuel cells: Mitigation of CO contamination," *IFAC-PapersOnLine*, vol. 49, no. 7, pp. 302–307, 2016.

[39] Y. Liu, W. Lehnert, H. Janßen, R. C. Samsun, and D. Stolten, "A review of high-temperature polymer electrolyte membrane fuel-cell (HT-PEMFC)-based auxiliary power units for diesel-powered road vehicles," *J. Power Sources*, vol. 311, pp. 91–102, 2016.

[40] X. Cheng *et al.*, "A review of PEM hydrogen fuel cell contamination: Impacts, mechanisms, and mitigation," *J. Power Sources*, vol. 165, no. 2, pp. 739–756, 2007.

[41] MAN Diesel & Turbo, Augsburg, Germany, "Soot deposits and fires in exhaust gas boilers," 2014. [Online]. Available: http://marine.man.eu/docs/librariesprovider6/technical-papers/soot-depo sits-and-fires-in-exhaust-gas-boilers.pdf?sfvrsn=23

[42] J. Pasel, R. C. Samsun, R. Peters, and D. Stolten, "Fuel processing of diesel and kerosene for auxiliary power unit applications," *Energy Fuel.*, vol. 27, no. 8, pp. 4386–4394, 2013.

[43] D. Vrančić, S. Strmčnik, and Đ. Juričić, "A magnitude optimum multiple integration tuning method for filtered PID controller," *Automatica*, vol. 37, no. 9, pp. 1473–1479, 2001.

[44] X. Yu, M. R. Starke, L. M. Tolbert, and B. Ozpineci, "Fuel cell power conditioning for electric power applications: A summary," *IET Elect. Power App.*, vol. 1, no. 5, pp. 643–656, 2007.

[45] P. Xuewei and A. K. Rathore, "Novel bidirectional snubberless naturally commutated soft-switching current-fed full-bridge isolated DC/DC converter for fuel cell vehicles," *IEEE Trans. Ind. Electron.*, vol. 61, no. 5, pp. 2307–2315, May 2014.
[46] S. Njoya Motapon, L. A. Dessaint, and K. Al-Haddad, "A comparative study of energy management schemes for a fuel-cell hybrid emergency power system of more-electric aircraft," *IEEE Trans. Ind. Electron.*, vol. 61, no. 3, pp. 1320–1334, Mar. 2014.
[47] K. R. Sree and A. K. Rathore, "Impulse commutated high-frequency soft-switching modular current-fed three-phase DC/DC converter for fuel cell applications," *IEEE Trans. Ind. Electron.*, vol. PP, no. 99, pp. 1–1, 2016.
[48] J. Chen, C. Xu, C. Wu, and W. Xu, "Adaptive fuzzy logic control of fuel-cell-battery hybrid systems for electric vehicles," *IEEE Trans. Ind. Informat.*, vol. PP, no. 99, pp. 1–1, 2016.
[49] A. Emadi, S. S. Williamson, and A. Khaligh, "Power electronics intensive solutions for advanced electric, hybrid electric, and fuel cell vehicular power systems," *IEEE Trans. Power Electron.*, vol. 21, no. 3, pp. 567–577, May 2006.
[50] Z. J. Shen, S. P. Robb, F. Y. Robb, M. Fuchs, D. Berels, and K. Hampton, "Load dump protection in 42 V automotive electrical distribution systems," in *Proc. 16th Annu. IEEE Appl. Power Electron. Conf. Expo.*, 2001, pp. 289–295.
[51] B. Wen, D. Sarafianos, R. A. McMahon, and S. Pickering, "Understanding automotive electrical network voltage transients," in *Proc. 8th IET Int. Conf. Power Electron., Mach. Drives*, 2016, pp. 1–6.
[52] *Road vehicles – Environmental conditions and testing for electrical and electronic equipment – Part 2: Electrical loads*, ISO 16750-2:2010(E), Geneva, Switzerland, 2010.

Boštjan Pregelj received the Ph.D. degree in electrical engineering from the Faculty of Electrical Engineering, University of Ljubljana, Ljubljana, Slovenia, in 2009.

Since 2004, he has been with the Jožef Stefan Institute, Ljubljana, Slovenia. He has been involved in a number of national, EU FP, and Horizon Research Projects, recently, also as the Coordinator of the FP7 FCGEN Project. He has extensive experience in advanced control algorithms, supervisory control, MPC, and hybrid systems, as well as with modeling, and simulation of such systems. Since 2009, his research has been predominantly oriented toward fuel cell and reformer systems, with control, modeling, and power management in the spotlight. Currently, he is also working on the development of fast MPC for ITER plasma control.

Andrej Debenjak (M'11) received the B.Sc. degree in electrical engineering from the Faculty of Electrical Engineering, University of Ljubljana, Ljubljana, Slovenia, and the Ph.D. degree in information and communications technology from the Jožef Stefan International Postgraduate School, Ljubljana, Slovenia, in 2011 and 2015, respectively.

He is currently a Postdoctoral Research Associate in the Jožef Stefan Institute. His research interests include fault detection and diagnostics of PEM fuel cell systems, and prognostics and health management of lithium-based batteries. Areas of his expertise include embedded programming, digital signal processing, statistical analysis, and diagnostics algorithm design.

Gregor Dolanc received the Ph.D. degree in electrical engineering from the Faculty of Electrical Engineering, University of Ljubljana, Ljubljana, Slovenia, in 2000.

He works in the field of general process control and automation, where he focuses on combining research and application-oriented work. His research is focused on process modeling, identification, and advanced control. He is strongly involved in industrial projects from various branches including machine building, the brick and tile industry, chemical industry, steel production industry, aircraft guidance and control, industrial diagnostic systems, and district heating testing systems. He has also been participating in several projects, FP and H2020, financed by the European Commission.

Janko Petrovčič received the Ph.D. degree in electrical engineering from the Faculty of Electrical and Computer Engineering, University of Ljubljana, Ljubljana, Slovenia, in 1992.

In 1983, he joined the Jožef Stefan Institute, Ljubljana, Slovenia, and since then he has been working in the Department of Systems and Control. He is currently an R&D advisor, and is working on EU's FP7 Projects, concerning the application of fuel cell-based power systems. His main activities are in the fields of process control engineering, process control algorithms, industrial diagnostics, signal acquisition, and electronic design. He works mainly on research and development projects for industry and is responsible for the hardware support of basic research activities of the department. He led the design of several industrial diagnostic systems for vacuum cleaner and EC motors for the Domel company, and participated in the design of BLDC-driven valve actuators for the Danfoss Trata company.